Molecular Biology of the Cell
Vol. 17, 3242–3253, July 2006

Dynein-dependent Motility of Microtubules and Nucleation Sites Supports Polarization of the Tubulin Array in the Fungus *Ustilago maydis*

Gero Fink and Gero Steinberg

Max-Planck-Institut für terrestrische Mikrobiologie, D-35043 Marburg, Germany

Submitted December 8, 2005; Revised April 21, 2006; Accepted April 24, 2006
Monitoring Editor: Yixian Zheng

Microtubules (MTs) are often organized by a nucleus-associated MT organizing center (MTOC). In addition, in neurons and epithelial cells, motor-based transport of assembled MTs determines the polarity of the MT array. Here, we show that MT motility participates in MT organization in the fungus *Ustilago maydis*. In budding cells, most MTs are nucleated by three to six small and motile γ-tubulin–containing MTOCs at the boundary of mother and daughter cell, which results in a polarized MT array. In addition, free MTs and MTOCs move rapidly throughout the cytoplasm. Disruption of MTs with benomyl and subsequent washout led to an equal distribution of the MTOC and random formation of highly motile and randomly oriented MTs throughout the cytoplasm. Within 3 min after washout, MTOCs returned to the neck region and the polarized MT array was reestablished. MT motility and polarity of the MT array was lost in dynein mutants, indicating that dynein-based transport of MTs and MTOCs polarizes the MT cytoskeleton. Observation of green fluorescent protein-tagged dynein indicated that this is achieved by off-loading dynein from the plus-ends of motile MTs. We propose that MT organization in *U. maydis* involves dynein-mediated motility of MTs and nucleation sites.

INTRODUCTION

The spatial organization and polarity of eukaryotic cells largely depends on their interphase microtubule (MT) arrays and associated proteins (Mandelkow and Mandelkow, 1995; Lane and Allan, 1998). MTs are tubulin polymers that possess an intrinsic polarity (Desai and Mitchison, 1997). Their minus-end is usually embedded in a microtubule-organizing center (MTOC), whereas most tubulin exchange occurs at the dynamic plus-end. The polarity of MTs is used by two opposing types of motor complexes, plus-end–directed kinesins and minus-end–directed dyneins (Hirokawa, 1998; Karki and Holzbaur, 1999; Vale, 2003) that move organelles and other "cargo" along MTs. The specific activity of these opposing motors participate in numerous essential processes, such as spindle formation and chromosome segregation (Sharp *et al*., 2000; Karsenti and Vernos, 2001; Gadde and Heald, 2004), organization of the endomembrane system (Lippincott-Schwartz *et al*., 1995; Burkhardt, 1998; Lane and Allan, 1998; Lippincott-Schwartz, 1998; Lane and Allan, 1999), and dynamic rearrangement of granules in melanophores (Gross *et al*., 2002; Barral and Seabra, 2004) or endosomes in fungal cells (Wedlich-Soldner *et al*., 2002b). Motors use the given polarity of the MT array that is usually determined by the cellular localization of the MTOC. Thus, the localization of the MTOC is a key factor in MT-based cellular organization. In addition, for animal cells it is known that other mechanisms, such as treadmilling of MTs (Rodionov and Borisy, 1997a; Maly and Borisy, 2002) or directed transport of assembled MTs (Keating *et al*., 1997; Rodionov and Borisy, 1997b; Mogensen, 1999) participates in the organization of the MT array. In particular in neurons MTs are highly motile (Tanaka and Kirschner, 1991; Dent *et al*., 1999; Yu *et al*., 2001). These MTs are released from the MTOC within the cell body (Yu *et al*., 1993) and actively transported into the axon (Baas and Ahmad, 1993). This process is known as slow axonal transport (Baas and Buster, 2004), and it is mediated by cytoplasmic dynein (Ahmad *et al*., 1998; He *et al*., 2005) that most likely is anchored to the cortex by interacting with F-actin (Garces *et al*., 1999; Hasaka *et al*., 2004). In contrast, the combined activity of kinesins and dynein leads to an anti-polar MT orientation in dendrites (Sharp *et al*., 1997a; Yu *et al*., 1997; Baas and Buster, 2004). Thus, in neurons MT orientation mainly results from the activity of motor complexes, whereas the site of MT nucleation is of minor importance for the organization of the MT arrays in these cells.

In yeast-like cells of the fungus *Ustilago maydis*, MT organization is thought to be determined by cell cycle-specific activation of cytoplasmic and nuclear MTOCs (Steinberg *et al*., 2001; Straube *et al*., 2003). In unbudded cells in G_1 or S phase, MTs are nucleated at numerous cytoplasmic sites and organize themselves into antipolar bundles (Straube *et al*., 2003). In contrast, budding cells in G_2 phase contain an almost unipolar MT cytoskeleton, with plus-ends reaching to the distal cell pole and into the growing bud. The polarization of MTs is thought to be based on the activity of MTOCs that are located in the neck region between the mother and the daughter cell (Straube *et al*., 2003). Interestingly, MTs within the interphase array are highly dynamic and undergo numerous types of motility, including bending

This article was published online ahead of print in *MBC in Press* (http://www.molbiolcell.org/cgi/doi/10.1091/mbc.E05–12–1118) on May 3, 2006.

The online version of this article contains supplemental material at *MBC Online* (http://www.molbiolcell.org).

Address correspondence to: Gero Steinberg (gero.steinberg@staff.uni-marburg.de).

Abbreviations used: GFP, green fluorescent protein; LatA, latrunculin A; MT, microtubule; MTOC, microtubule organizing center; RFP, red fluorescent protein; YFP, yellow fluorescent protein.

and sliding (Steinberg *et al*., 2001). In addition, free MTs are transported along the cortex at rates that are reminiscent of motor activity (Steinberg *et al*., 2001). However, neither the motor for this MT motility nor the cellular importance for MT transport in *U. maydis* is known. Here, we demonstrate that cytoplasmic dynein mediates transport of individual MTs and nucleation sites. This motility is essential for MT polarization, suggesting that motor activity organizes MTs in growing *U. maydis* cells.

MATERIALS AND METHODS

Strains, Plasmids, and Growth Conditions

Cloning methods followed standard protocols, and DNA transformation was done as described previously (Schulz *et al*., 1990). To visualize MT plus-ends in the green fluorescent protein (GFP)-α-tubulin–expressing strains FB2_GT (Steinberg *et al*., 2001) and FB1Dyn2^{ts}_GT (Adamikova *et al*., 2004), the endogenous copy of *peb1*, an EB1-homologue in *U. maydis* (Straube *et al*., 2003), was replaced by a construct containing monomeric red fluorescent protein (RFP) (Campbell *et al*., 2002) C-terminally fused to *peb1* that was followed by a phleomycine resistance cassette. In addition, a Peb1-yellow fluorescent protein (YFP) fusion construct (Straube *et al*., 2003) was homologously integrated into the temperature-sensitive dynein mutant strain FB1Dyn2^{ts} (Wedlich-Soldner *et al*., 2002a). To analyze the relationship between the polar MTOC and the nucleus, the Peb1-YFP construct and GFP fused to a nuclear localization signal (Straube *et al*., 2001) were integrated into strain the wild-type strain FB2 (Banuett and Herskowitz, 1989; Table 1). All homologous integration events were confirmed by Southern blotting. All strains were grown at 28°C in complete medium supplemented with 1% glucose (CM-G; Holliday, 1974) and solid media contained 2% (wt/vol) bacto-agar. Temperature-sensitive (ts) *dyn2*^{ts} strains and corresponding control strains were grown overnight at 22°C and incubated in a 31–32°C water bath for restrictive growth.

Light Microscopy and Image Processing

Microscopic analysis was performed using a Axioplan II microscope (Carl Zeiss, Oberkochen, Germany). Epifluorescence was observed using standard fluorescein isothiocyanate, 4,6-diamidino-2-phenylindole, and rhodamine filter sets. Video sequences of Peb1-RFP– and GFP-labeled MTs were taken with a filter wheel (Ludl Electronics, Hawthorne, NY), equipped with specific excitation filters (GFP, BP480/25; DsRed, BP 565/25) and a dual band mirror (eGFP, FT 480, BP503–545; DsRed, FT565, BP591-647; AHF Analysetechnik, Tübingen, Germany). Frames were taken with either a cooled C4742-95 camera (Hamamatsu, Herschingen, Germany) controlled by Image-Pro Plus (Media Cybernetics, Silver Spring, MD) or a CoolSNAP-HQ charge-coupled device camera (Photometrics, Tucson, AZ) controlled by the imaging software MetaMorph (Molecular Devices, Downington, PA). All quantification and image processing, including two-dimensional deconvolution, *z*-axis maximum projection, and adjustment of brightness, contrast, and γ-values was done in Image-Pro Plus, MetaMorph, or Photoshop (Adobe Systems, Mountain View, CA).

Speckle Analysis and Monitoring Microtubule Orientation

Speckle analysis was done using strain FB2rGFPTub1 (Steinberg *et al*., 2001). Grown in complete medium supplemented with 1% arabinose (CM-A), this strain expresses an additional copy of α-tubulin that is fused to GFP. After shift to complete medium supplemented with 1% glucose, the *crg*-promoter is repressed (Bottin *et al*., 1996), and the amount of GFP-α-tubulin gradually decreases with time, which results in GFP speckles in the MTs after ~4 h in glucose. Quantitative linescan analysis was done using MetaMorph. MT orientation was investigated by following Peb1-RFP or Peb1-YFP fusion proteins in control or temperature-sensitive dynein strains (Table 1). Image series were taken at 1- to 1.5-s time interval, and the motility of Peb1 signals was monitored. Because Peb1 only binds to growing MT plus-ends (Straube *et al*., 2003), moving signals indicated MT elongation and thus orientation. For experiments using a temperature-sensitive dynein allele (*dyn2*^{ts}; Wedlich-Soldner *et al*., 2002a), control cells and dynein mutants were cultivated overnight at 22°C and than shifted to a 31–32°C water bath for 70–90 min. Budding cells were microscopically observed using a temperature-adjustable 100× Apochromat objective that was prewarmed at 32°C.

Benomyl Experiments

Benomyl-induced depolymerization was monitored by placing 1 μl of logarithmically growing FB1GT cells on a 2% agar/20 or 30 μM benomyl cushion that was generated by flattening 100 μl of hot agar solution between two microscope slides. Depolymerization of MTs was immediately observed in the microscope, and *z*-axis stacks were taken at various time points. For benomyl recovery experiments, 5 ml of logarithmically growing cells was incubated with 20 μM benomyl (Sigma Chemie, Taufkirchen, Germany) for 30–90 min at 28°C, and disruption of GFP-MTs was microscopically checked. Three hundred microliters of the benomyl-containing suspension was sedimented at 3500 rpm for 10 s. The pellet was resuspended in 300 μl of fresh medium, and cells were rapidly sedimented at 3500 rpm for 5–10 s. After removal of the supernatant, cells were resuspended in 100 μl of fresh medium, embedded in low-melt agarose, and immediately observed under the microscope. For recovery experiments on temperature-sensitive dynein mutants, all media, the centrifuge, and the microscope objective were prewarmed to ~32°C. Image stacks of budded cells were acquired for 200 ms at ~300-nm *z*-axis steps before benomyl treatment and within 6 min after drug removal.

Quantitative Analysis of γ-Tubulin-GFP Distribution

Strain FB1rTub2_T2G_R$_2$T1 contained 1) the endogenous copy of the γ-tubulin gene *tub2* under the control of the repressible *crg* promoter, 2) an ectopic copy of tub2 fused to GFP, and 3) a double RFP fused to α-tubulin (*tub1*). Cells were grown in CM-A, and tub2 expression was repressed after shift to CM-G for 4 h. Tub2-GFP that were visible for at least 1.5 s (3 frames) were counted in the neck region that was defined as the area ± 3.5 μm around the neck constriction and compared with the number of Tub2-GFP dots within the rest of the cytoplasm. All values were normalized to an area of 1 μm^2.

RESULTS

Many Interphase Microtubules Have No Contact with the Neck Region

Yeast-like cells of *U. maydis* grow by polar budding. The daughter cell (Figure 1A, indicated by D) is separated from the mother (Figure 1A, indicated by M) by a cell constriction (Figure 1A, indicated by neck). In strain FB2GT that expresses a fusion protein of GFP and Tub1, the α-tubulin of *U. maydis* (Steinberg *et al*., 2001; for strains, see Table 1), *z*-axis projections of six to eight optical planes demonstrated that long MTs are focused at the neck region (Figure 1A, arrowheads) and extend into the mother and the daughter cell. In addition, many cells contained short MTs that had no contact with the neck region (Figure 1A, arrow). To monitor the orientation of MTs in this array, we labeled MTs with GFP-α-tubulin and the plus-ends with a fusion protein of RFP and Peb1, an EB1-homologue that binds to MT plus-ends in *U. maydis* (Straube *et al*., 2003; strain FB2Peb1R_GT; also see Table 1). Consistent with previous results, we found that Peb1-RFP localized to elongating MT plus-ends that grew toward the distal cell pole, but it was absent from rapidly shortening MTs (Figure 1B, arrowhead in series). Occasionally, we observed that two Peb1-labeled plus-ends occurred at the same site in the neck and left the site in opposite directions (Figure 1C, arrows in image series; enlarged area indicated by box). This supports the notion that the neck region contains MTOCs (Straube *et al*., 2003). This nucleation activity was not associated with the nuclear spindle pole body, because the nucleus, marked with GFP fused to a nuclear localization signal (Straube *et al*., 2001), was located in the mother cell (Figure 1C, strain FB2Peb1R_nGFP). A detailed quantitative analysis of the orientation of MTs revealed that yeast-like cells (strain FB2Peb1R_GT) contain three classes of MTs: 1) long MTs that reach into neck region (Figure 1D, 1), 2) short MTs that were in contact with these long MTs (Figure 1, 2), and short "free" MTs (Figure 1D, 3). Whereas MTs of class 1 extend 96.5% of their plus-ends to the cell poles, MTs of the other classes had a more random orientation, with 57.4 (class 2) and 42.2% (class 3) of all plus-ends directed to the cell poles.

To gain more direct evidence for a role of polar MTOCs in MT organization, we developed an assay, in which we placed GFP-α-tubulin–expressing cells on top of an agar cushion supplemented with benomyl, a fungicide that reversibly destroys the tubulin cytoskeleton in *U. maydis* (Straube *et al*., 2003; Fuchs *et al*., 2005). This experimental setting allowed the microscopic observation of MT depoly-

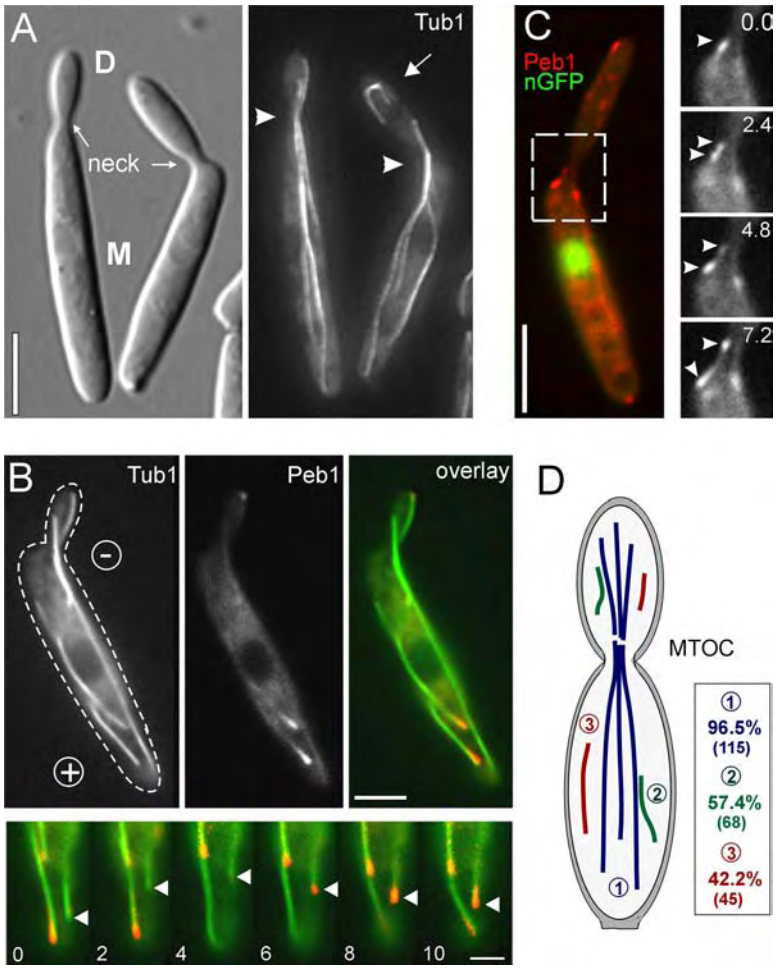

Figure 1. Organization of the MT cytoskeleton in budding cells of *U. maydis*. (A) In growing cells of *U. maydis*, most MTs, labeled by GFP-α-tubulin of *U. maydis* (Tub1; Steinberg *et al.*, 2001), are focused at the constriction (neck, arrowheads in left panel) between the mother (M) and the daughter (D) cell, where polar MTOCs are thought to participate in organizing the interphase MT array (Straube *et al.*, 2003). In addition, short MTs without contact with the neck region are also visible (right, arrow). Note that MT images are *z*-axis projection of six to eight optical planes. Bar, 5 μm. (B) Coexpression of GFP-α-tubulin (Tub1, green in overlay) and Peb1-RFP (Peb1, red in overlay) confirms that the EB1-homologue labels growing MT tips, whereas it is absent from shrinking MTs (arrowhead in image series). Elapsed time is given in second. Bars, 3 μm in overview and 2 μm in image series. See Supplemental Video material. (C) The simultaneous appearance of Peb1-RFP (Peb1)–labeled MT plus-ends at single sites within the neck region (arrowheads in series) indicates that MTs are nucleated at a cytoplasmic MTOC (Straube *et al.*, 2003). Expression of GFP fused to a nuclear localization signal (nGFP) demonstrates that the nucleation of MTs, indicated by the simultaneous appearance of plus-ends at one site, is independent of the nuclear spindle pole body. Elapsed time is given in seconds. Bar, 5 μm. (D) Budded cells of *U. maydis* strain FB2Peb1R_GT contain three classes of MTs. Most MTs have contact with the neck region (1, blue), and 96.5% of the MTs extend their plus-ends to the cell poles. In contrast, shorter MTs that either are associated to longer MTs (2, green) or were without contact with other MTs (3, red) showed an almost random orientation. Number of plus-ends directed to the cell poles is given in box; sample size is indicated in parentheses.

merization in real time. Under the assumption that most MTs are nucleated at polar MTOCs, we predicted that minus-ends of shrinking MTs would keep contact with the neck region while they depolymerize at their plus-ends. Indeed, MTs disappeared within 6 min under benomyl treatment (Figure 2A, 6:00 min). Consistent with our model, most long MTs were still in contact with the neck region when incubated for 1–3 min (Figure 2A, 1:15 and 2:15 min; arrowhead marks neck region). However, additional free MTs that were not in contact with the polar MTOC were frequently found (Figure 2A, arrow at 2:15 min). A quantitative analysis revealed that about one-half of all cells contained such short MTs, suggesting that free MTs are a regular part of the MT array of *U. maydis*. To investigate this further, we performed benomyl recovery experiments, in which MTs were depolymerized in the presence of 20 μM benomyl (Figure 2B, +ben), and their reappearance was monitored after washout of the drug. Indeed, 1–2 min after rinsing the cells with fresh medium, MTs occurred randomly in the mother cell (Figure 2B, arrow), suggesting that MTs were nucleated at cytoplasmic nucleation sites. To determine the orientation of these free MTs, we performed benomyl recovery experiments using strain FB2Peb1R_GT. These experiments surprisingly revealed that reappearing MTs initially had a random orientation, with almost 50% of all MT plus-ends growing to the distal cell pole (Figure 2C, 1.5 min after washout of the drug). However, with time the MT array rapidly repolarized and the normal degree of polarization was achieved ~3–3.5 min after removal of the drug (Figure 2C, compare 3.5 min and untreated).

Microtubules Undergo Unidirectional Motility

Our results indicated that a considerable portion of MTs is nucleated at free sites in the cytoplasm of the mother cell. Interestingly, repolarization of the MT array was accompanied by a significant increase of MT motility (Figure 3A), and even very short MTs were moving in cells that recovered from benomyl (Figure 3B), suggesting that MT motility participates in MT organization. Rapid motility of MTs at rates up to ~41 μm/min was previously described in interphase of *U. maydis* (Steinberg *et al.*, 2001). This phenomenon was found in ~5–8% of untreated cells of strain FB1GT, and MTs were often moving along the periphery of the cell (Figure 3C, arrows). To confirm that assembled MTs are transported, we performed a speckle analysis of this motility phenomenon. We made use of strain FB2rGFPTub1 that contains GFP-α-tubulin under the control of the inducible/repressible *crg*-promoter in addition to its endogenous α-tubulin (Steinberg *et al.*, 2001). Growing this strain under inductive conditions (see *Materials and Methods*), cells express GFP-Tub1, which is incorporated into the MTs. After shift to repressive conditions for ~4 h, the level of GFP-Tub1 decreases, and speckles of the fusion protein occur in interphase MTs. Formation of speckles is expected to be a random process; therefore, speckled MTs are most likely individually polymers. These speckles were used as struc-

Table 1. Strains and plasmids used in this study

Name	Genotype	Reference
FB2GT	*a2b2*/potefGFPTub1	Steinberg *et al.* (2001)
FB1GT	*a12b1*/potefGFPTub1	Steinberg *et al.* (2001)
FB2Peb1R_nGFP	*a2b2* P*peb1-peb1-mrfp*, *ble*^{R}/pnGFP	This study
FB2Peb1R_GT	*a2b2* P*peb1-peb1-mrfp*, *ble*^{R}/potefGFPTub1	Straube *et al.* (2005a)
FB2rGFPTub1	*a2b2*/prGFPTub1	Steinberg *et al.* (2001)
FB1rT2_T2G_R_2T1	*a1b1* P*crg-tub2*, *ble* P*otef-tub2-gfp*, *cbx*^{R}/pRFP$_2$Tub1	This study
FB1rT2_T2G_P1R	*a1b1* P*crg-tub2*, *ble* P*otef-tub2-gfp*, *cbx*^{R}, P*peb1-peb1-mrfp*, *nat*^{R}	This study
FB1Dyn2^{ts}GT	*a1b1* P*dyn2-dyn2*^{ts}, *nat*^{R}/potefGFPTub1	Adamikova *et al.* (2004)
FB2G$_2$Dyn1_RT	*a2b2* P*dyn1-2* × *gfp-dyn1*, *hyg*^{R}/pRFPTub1	Straube *et al.* (2005b)
FB2G$_2$Dyn1_RT	*a2b2* P*dyn1-2* × *gfp-dyn1*, *hyg*^{R}/pRFPTub1	(Straube *et al.* (2005b)
FB1Dyn2^{ts}_P1R_GT	*a1b1* P*dyn2-dyn2*^{ts}, *nat*^{R} *peb1-mrfp*, *ble*^{R}/potefGFPTub1	This study
FB2Peb1Y	*a1b1* P*peb1-peb1-yfp*, *ble*^{R}	Straube *et al.* (2003)
FB1Dyn2^{ts}_P1Y	*a1b1* P*dyn2-dyn2*^{ts}, *nat*^{R} *peb1-yfp*, *ble*^{R}	This study
pnGFP	P*otef-gal4(s)-sgfp*, *cbx*^{R}	Straube *et al.* (2001)
potefGFPTub1	P*otef-egfp-tub1*, *cbx*^{R}	Steinberg *et al.* (2001)
prGFPTub1	P*crg-egfp-tub1*, *cbx*^{R}	Steinberg *et al.* (2001)
pRFPTub1	P*otef-mrfp-tub1*, *cbx*^{R}	Straube *et al.* (2005b)
pRFP$_2$Tub1	P*otef-mrfp-mrfp-tub1*, *hyg*^{R}	This study

a, *b*, mating type loci; P, promoter; -, fusion; *ble*^{R}, phleomycin resistance; *cbx*^{R}, carboxin resistance; *nat*^{R}, nourseothricin resistance; /, ectopically integrated; *gal4(s)*, nuclear localization signal of the GAL-4 DNA binding domain from pC-ACT1 (Clontech, Mountian View, CA); *egfp*, enhanced green fluorescent protein; *yfp*, yellow-shifted fluorescent protein; *mrfp*, monomeric red fluorescent protein; *dyn1/dyn2*: N-/C-terminal half of the dynein heavy chain; *tub1*: alpha-tubulin; *peb1*, EB1-like plus-end binding protein; *otef*, constitutive promoter; and *crg*, sugar-sensitive inducible/repressible promoter.

tural landmarks on moving MTs. In all cases of MT motility that were observed, these speckles remained constant while the MT was translocated (Figure 3D, arrowheads; compare with stationary signals marked by asterisk; and E, arrows). This strongly indicates that assembled MTs are transported by unknown motor activity. This transport is a frequent process, because >50% of all free or bundled MTs showed either directed motility or bending within 30-s observation time (Table 2, motility), and both populations undergo either polymerization or depolymerization (Table 2, dynamic instability).

Microtubules Are Nucleated at Numerous Cytoplasmic Sites

Interestingly, we found that some motile MT structures showed Peb1-RFP staining at both ends (Figure 4, A1 and A2, arrows; strain FB2Peb1R_GT), indicating that they consist of two MTs of opposite orientation that emanate from a bipolar MTOC. Indeed, a small, less fluorescent region was occasionally found near the middle of both MT plus-ends (Figure 4B1 and B2; asterisk; also see Figure 5A). This region was flexible and could function as a hinge in bending MTs (Figure 4B2, arrow indicates bending direction; interval between both images is ~2.4 s). Based on the bipolarity of these MT structures and the unusual flexibility of the hinge, we speculate that the nonfluorescent structures are nucleation sites. To confirm this, we observed a fusion protein of γ-tubulin and GFP (Tub2-GFP), which is located at MTOCs in *U. maydis* (Straube *et al*., 2003). In strain FB1rT2_T2G_R_2T1, grown for 4 h in CM-G, the endogenous

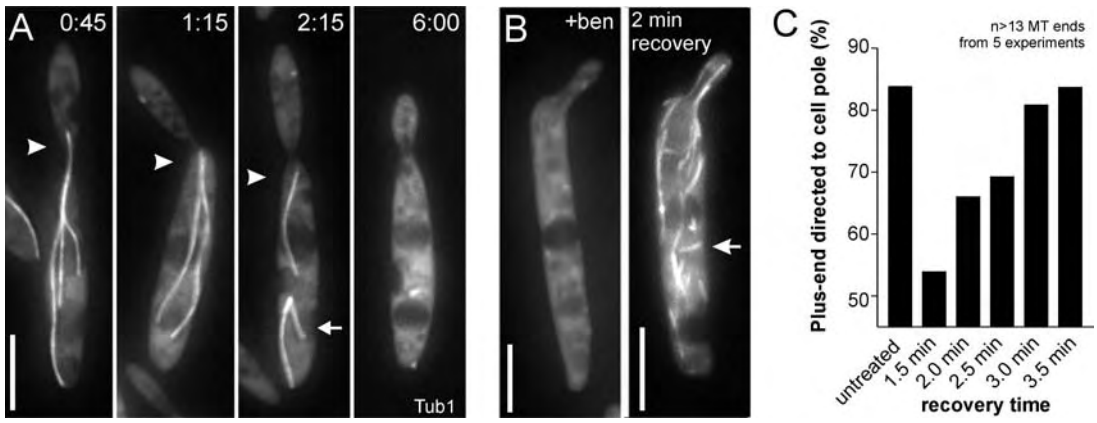

Figure 2. Free MTs in interphase cells of *U. maydis*. (A) Controlled depolymerization of MTs was achieved by placing cells on an agar cushion that contains 30 μM benomyl. As the drug diffuses into the cell, MTs rapidly depolymerize toward their origin at the neck region (arrowhead). However, free MTs are commonly seen (arrow). All MTs disappear after ~6-min drug treatment. Elapsed time after exposure to benomyl is given in minutes:seconds. Bar, 5 μM. (B) Treatment of GFP-Tub1–expressing cells with 20 μM benomyl for 30 min efficiently depolymerizes MTs (+ben). Rinsing these cells wish fresh medium (2 min, recovery) leads to a rapid reappearance of MTs within the cytoplasm of the cell (arrow). Bar, 3 μm. (C) In benomyl recovery experiments at 28°C using strain FB2Peb1Y_GT, newly appearing MTs have a random orientation (1.5-min recovery time), but they rapidly repolarize within ~4 min (recovery time, time after washout of benomyl).

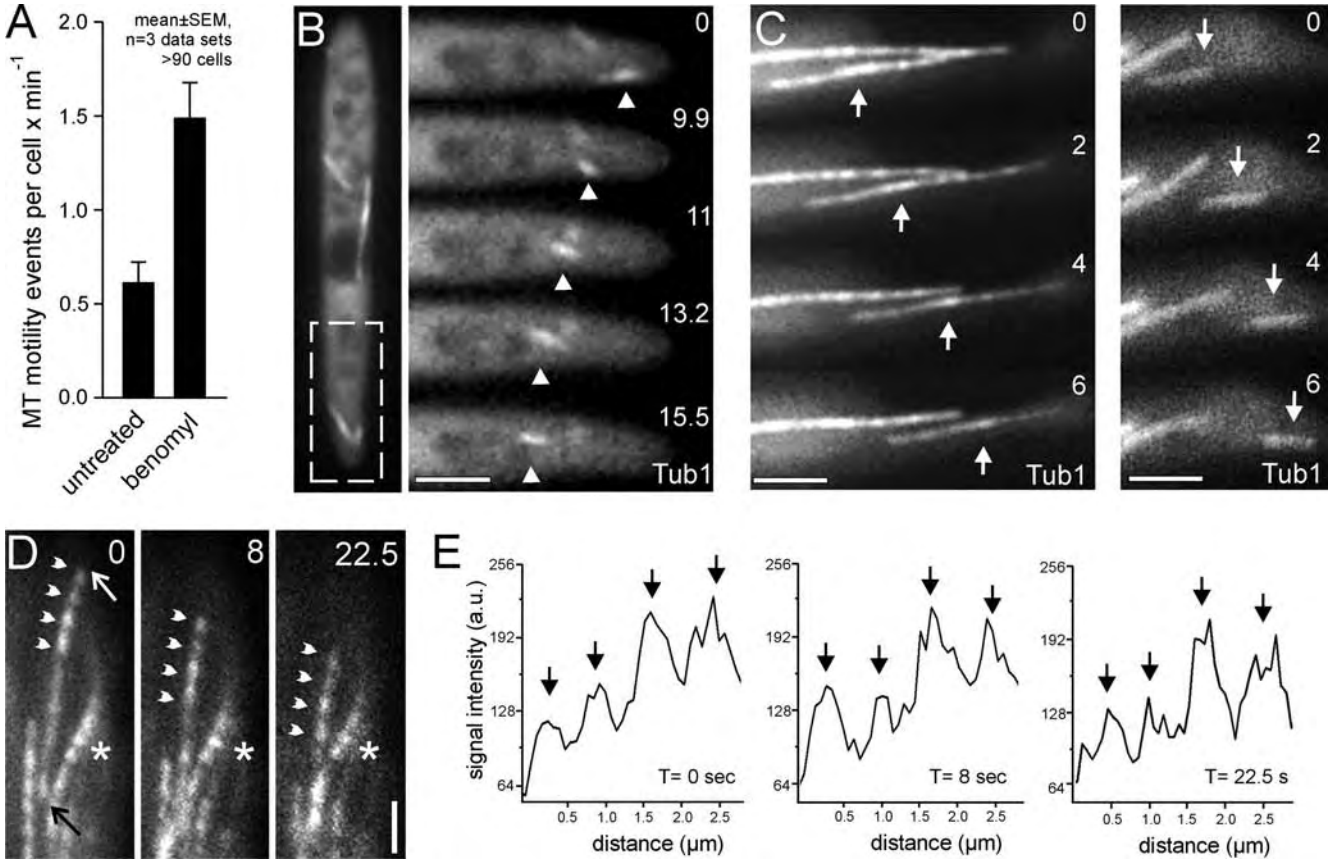

Figure 3. Microtubule motility in *U. maydis*. (A) Motility was rarely found in untreated cells (32°C). However, after benomyl treatment and washout of the drug, numerous short MTs are formed and motility was drastically increased. MT motility is given as MT motility events × min^{-1}. (B) Immediately after removal of benomyl, short MTs reappeared that often moved throughout the cytoplasm (arrowhead). Enlarged area indicated by box in overview. Elapsed time is given in seconds. Bar, 2 μm. See also Supplemental Video material. (C) Motion of MTs along the cortex of the cell. Motility happens at rates up to ~41 μm/min (Steinberg *et al.*, 2001), indicating that it is motor-based. Elapsed time is given in seconds. Note that cortical MT transport occurs independently of other MTs. Elapsed time is given in seconds. Arrows mark moving MTs. Bars, 2 μm. (D) Speckle analysis of MT motility. Gradual decrease of GFP-α-tubulin in a strain that also expresses endogenous unlabeled α-tubulin results in an unequal incorporation of GFP-α-tubulin and fluorescent speckles (arrowheads). These landmarks maintain their position while the MT moves, indicating that motility is due to transport of the assembled MT rather than treadmilling. Ends of the moving MT are indicated by arrows, a stationary reference point is marked by asterisks. Bar, 1.5 μm. See Supplemental Video material. (E) Linescan analysis of GFP-α-tubulin intensities in a moving MT confirms that speckles (arrows) remain unchanged during MT motility.

copy of *tub2* is repressed and Tub2 is replaced by Tub2-GFP fusion protein (Straube *et al.*, 2003). Under these conditions, faint Tub2-GFP dots were seen at the nonfluorescent hinge of the bend MT structures (Figures 4C, arrow, and 5A). In addition, γ-tubulin-GFP was found at the end of moving MTs (our unpublished data), suggesting that both MTs and nucleation sites are transported. Simultaneous observation of Tub2-GFP and Peb1-RFP in strain FB1rT2_T2G_P1R confirmed that one or two plus-ends leave these γ-tubulin dots, suggesting that they are indeed sites of MT nucleation (Figure 4D, arrow). Three to four of these Tub2-GFP dots were usually found in the neck region of budding cells (Figure 5A, arrowheads, strain FB1rT2_T2G_R_2T1). Interestingly, the γ-tubulin signals, together with short MTs (Figure 5A, details), were motile and showed frequent short-distance movements toward the bud (Figure 5B, arrow; series shows motility of TUB2-GFP dot shown at the bottom of Figure 5A). In addition, they suddenly occurred at the neck, which could be due to new formation of MTOCs or their appearance from regions not in the focal plane (Figure 5B, compare first frame with 2 signals and last frame with 4 dots; see also inset in Figure 5C). Concentration of Tub2-GFP was only seen in the neck of budding cells (Figure 5C, asterisk), indicating that the polar MTOC consists of numerous small and motile nucleation sites. Interestingly, the polar MTOC accumulation at the neck was lost after disruption of MTs with benomyl, and Tub2-GFP dots were randomly distributed (Figure 5D, arrows; spindle pole body indicated by arrowhead; neck indicated by asterisk). However, 3–4 min after washout of the MT inhibitor, Tub2-GFP dots reappeared

Table 2. Microtubule dynamics

	% Motility	% Dynamic instability	Sample size
Free MTs[a]	55.4	77.8	9
Bound MTs[b]	62.5	50	24

[a] Bending and sliding.
[b] MTs in contact with other MTs.

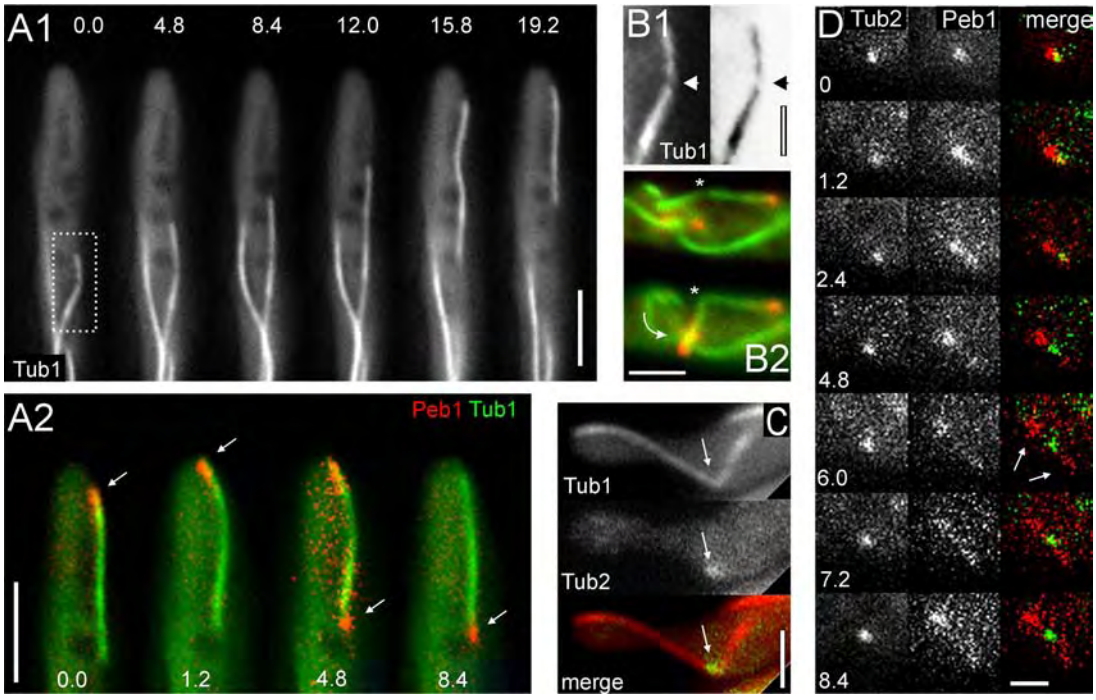

Figure 4. Cytoplasmic nucleation cites in budded cells. (A) In GFP-Tub1–expressing cells, MTs occasionally move along the cortex (A1). In most cases, plus-ends were labeled with a single Peb1-RFP signal, but some MT structures have two Peb1-binding growing plus-ends (A2, arrows), suggesting that these structures consist of two MTs that are connected by a nucleation site. Elapsed time is given in seconds. Bar, 5 μm. See Supplemental Video material. (B) In bipolar MT structures, a speckle of reduced fluorescence was often found near the middle of the bipolar MT structure (B1, arrowhead; example is taken from series in A1, area is indicated). The speckle is serves as a flexible hinge (asterisk; arrow indicates direction of bending motility; time interval ~2.4 s). Bar, 1 μm in B1 and 2 μm in B2. (C) A fusion of γ-tubulin (Tub2) and GFP locates to the tip of a buckled MT structure (arrows), suggesting that it consists of two MTs that emanate from a cytoplasmic MTOC. Bar, 2 μm. (D) Simultaneous observation of Tub2-GFP and Peb1-RFP demonstrates that MT plus-ends (arrows) extend from the cytoplasmic nucleation sites. Elapsed time is given in seconds. Bar, 1 μm. See Supplemental Video material.

at the neck (Figure 5E), which nicely corresponds with the reappearance of the polarized MT array (see above; Figure 2C).

Dynein Drives Microtubule Motility

The results presented so far demonstrate that MTs and γ-tubulin–containing MTOCs move within the cell. Apparently, this motility concentrates MTOCs at the neck region and is therefore most likely responsible for the establishment of the polar MT array in budding cells. As a first step toward an understanding of the putative motor activity for MT transport, we set out to determine the orientation of moving MTs in strain FB2Peb1R_GT. Most of these free MTs carried a single Peb1-RFP signal and almost all MTs moved with their Peb1-RFP signal leading (Figure 6, A and C). Because Peb1-RFP marks growing plus-ends this result indicated that MTs slid as a consequence of the activity of a minus-directed motor that pushed the MT plus-end forward. In addition, MTs occasionally moved with the plus-end trailing behind (Figure 6C) or even showed a bidirectional to-and-fro motion (Figure 6B). This raises the possibility that unknown plus-directed motors also participate in MT motility. Studies in neurons and fibroblasts suggest that minus-end–directed cytoplasmic dynein mediates MT motility in animal systems. Thus, we speculated that dynein could be responsible for MT transport in *U. maydis*. To check this possibility, we investigated the motility of GFP-α-tubulin–labeled MTs after benomyl recovery in conditional dynein mutants (strain FB1Dyn2^{ts}_GT). This mutant contains a temperature-sensitive allele of *dyn2*, which encodes the C-terminal half of the dynein heavy chain in *U. maydis* (Straube *et al*., 2001). At the restrictive temperature for Dyn2^{ts} cells (Wedlich-Soldner *et al*., 2002a), benomyl-treated control cells showed prominent MT motility (Figure 7A, control; strain FB1GT). In contrast, in dynein mutants motility of free MTs was almost abolished, indicating that cytoplasmic dynein is the motor for MT motility in *U. maydis* (Figure 7A, Dyn2ts). Interestingly, MT motility was significantly impaired after disruption of F-actin by 20 μM latrunculin A (Figure 7B, +LatA), suggesting that some motility is mediated by an interaction of dynein with F-actin at the cortex. However, about one-half of all MT motility was still found in the absence of F-actin.

To gain further insight into the role of dynein in MT motility, we observed a GFP_2-Dyn1 fusion protein that was expressed from its endogenous *dyn1* locus in a strain that also contained RFP-α-tubulin–labeled MTs (strain FB2G_2Dyn1_RT; Table 1). The dynein motor complex localized to the tips of astral MTs in anaphase (Figure 7C, only half of an anaphase spindle is shown) and to MT plus-ends at the cell poles of interphase cells (Figure 7D, small bud shown), where it remains attached while MTs were shrinking (Figure 7D, arrow in series). Plus-ends of free MTs also accumulated dynein (Figure 7E1). On MT translocation, a minor fraction of dynein left the tip and dispersed along the length of all observed moving MTs (Figure 7E1, arrows), but it returned to the plus-end when the MT stopped moving

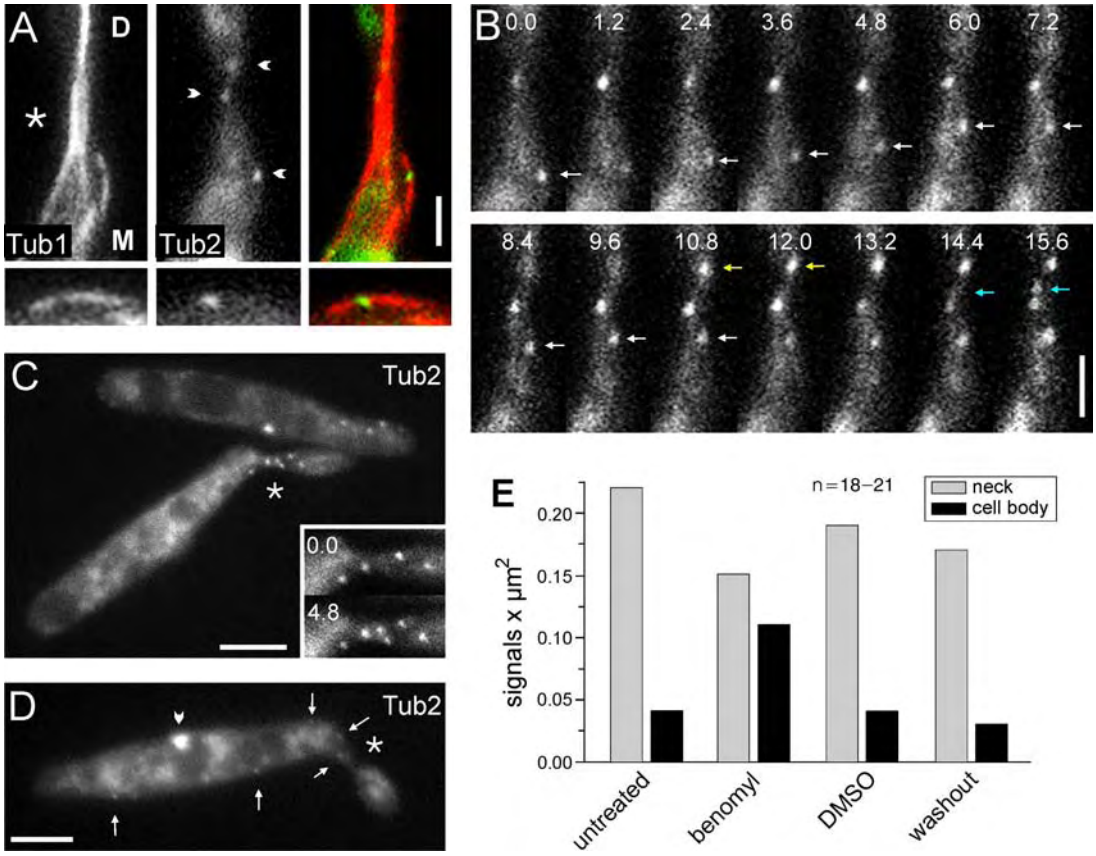

Figure 5. Motility of γ-tubulin–containing nucleation sites. (A) In strain FB1rTub2_GT2_R_2T1 MTs are stained by RFP-α-tubulin (Tub1), whereas γ-tubulin is fused to GFP (Tub2). Tub2-GFP dots (arrowheads) concentrate in the neck region (indicated by asterisk). The bottom signal colocalizes with a speckle (insets), indicating that these speckles are MTOCs. D indicates daughter cell, and M indicates mother cell. Bar, 2 μm. (B) Series from Figure 5A, showing motility of Tub2-GFP dots. A γ-tubulin signal moves toward the neck (white arrow). Two more signals occur during the course of observation. Elapsed time is given in seconds. Bar, 2 μm. See Supplemental Video material. (C) Overview showing the concentration of γ-tubulin dots (Tub2-GFP) in the neck region of a budded cell. Inset shows the dynamic behavior of the MTOCs in the neck. Elapsed time is given in seconds. Bar, 3 μm. (D) In benomyl, MTs are disrupted, and faint γ-tubulin-GFP signals are scattered within the cytoplasm (arrowheads). No accumulation is seen in the neck region (asterisk). The spindle pole body is indicated by arrowhead. Bar, 2 μm. (E) Quantitative analysis of the distribution of Tub2-GFP dots in untreated and benomyl-treated cells. Disruption of MTs abolishes the clustering of γ-tubulin signals in the neck (benomyl), whereas the solvent has no effect (DMSO). Three to 4 min after washout of the inhibitor, the array reappears, and the MTOCs concentrate in the neck region (washout).

(Figure 7E2, previous movement of MT is not shown; arrow marks dynein). Occasionally, distinct dynein signals were observed that remained stationary while the MT moved along the cell periphery (Figure 7E3, arrows), suggesting that MTs are sliding by dynein anchored to the cell cortex.

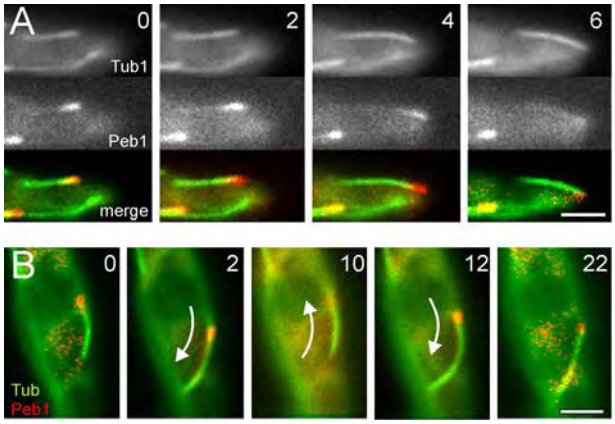

Figure 6. Direction of MT transport. (A) The plus-ends of growing MTs (Tub1) carry the EB1-homologue Peb1 fused to RFP (Peb1). This signal usually leads the moving MT, indicating that a stationary minus-end–directed motors pushes the tubulin polymer through the cytoplasm. Elapsed time is given in seconds. Bar, 2 μm. See also Supplemental Video material. (B) Occasionally, MT show a to-and-fro motility in both directions (arrows), suggesting that both, minus- and plus-end–directed motors support MT transport. Elapsed time is given in seconds. Bar, 2 μm. (C) Quantitative analysis of the direction of MT transport. In most cases, moving MTs carried a Peb1-RFP signal at the leading tip. Occasionally, no signal was seen or the Peb1-RFP cap was trailing behind. This indicates that most MT transport is based on minus-end–directed motors.

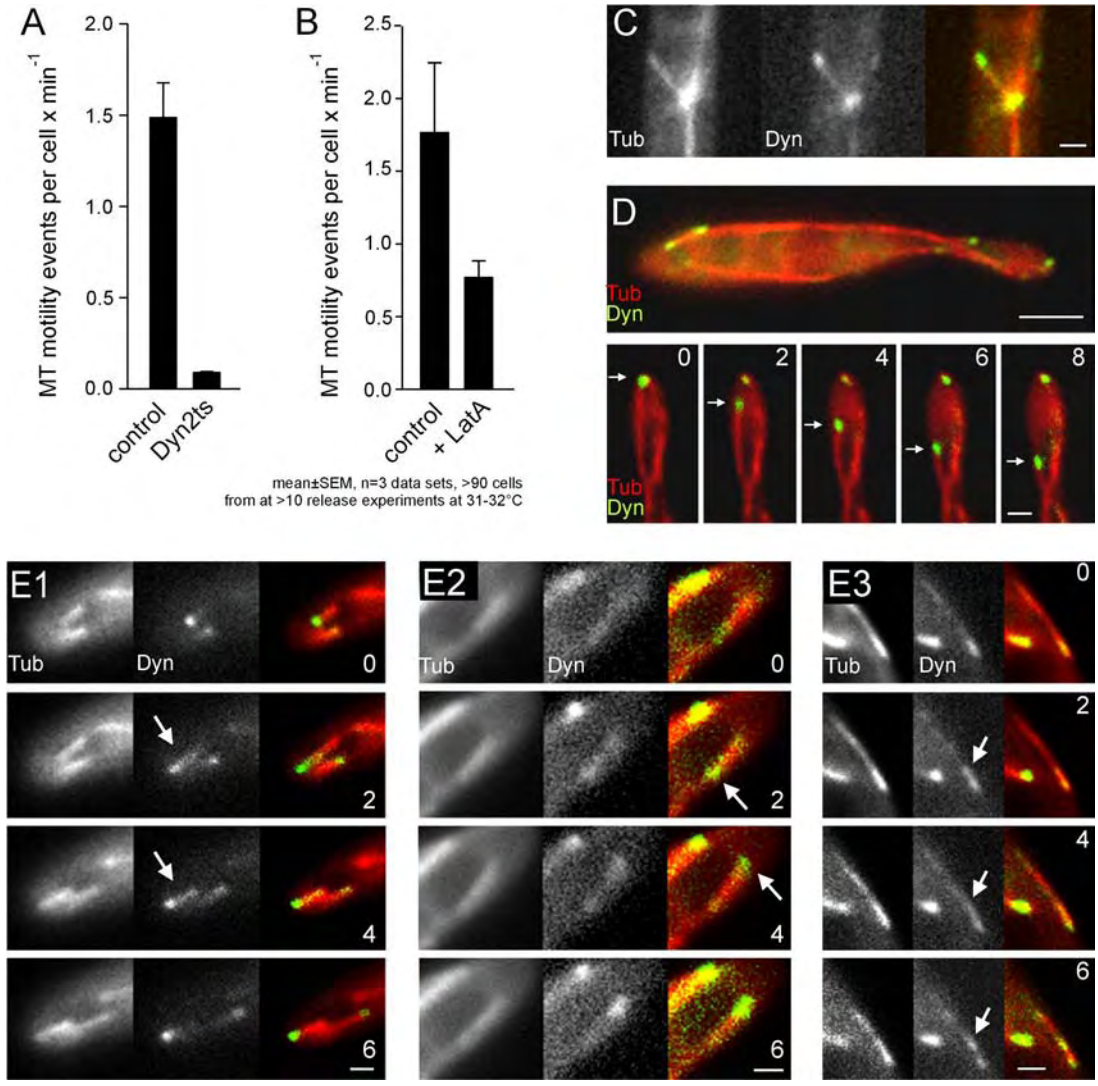

Figure 7. Microtubule motility and dynein. (A) In a temperature-sensitive dynein mutant (strain FB1Dyn2^{ts}_P1R_GT), inactivation of dynein at 31–32°C almost abolished MT motility (Dyn2ts). Note that this result nicely matches the portion of MTs that move with their pus-end leading (Figure 6C), suggesting that dynein is the assumed minus-motor for MT translocations. MT motility is given as MT motility events × min^{-1}. (B) Latrunculin A (20 μM) disrupts F-actin in *U. maydis* (Fuchs *et al.*, 2005), and this treatment inhibits ~50% of all MT motility after benomyl recovery. However, a significant portion of MT transport still occurs, suggesting that dynein can move MTs in the absence of F-actin. MT motility is given as MT motility events × min^{-1}. (C) A 2xGFP tag was fused to the N terminus of the endogenous *dyn1* gene. The GFP$_2$-Dyn1 fusion protein (Dyn) is biologically active and locates to the plus-ends of astral MTs in anaphase (Tub) that were labeled with RFP-α-tubulin. Tub, RFP-α-tubulin; Dyn, GFP$_2$-Dyn1. Bar, 1 μm. (D) GFP$_2$-Dyn1 locates to MT plus-ends in interphase, but in contrast to Peb1 remains at the MT end during rapid shrinkage of the tubulin polymer (arrow in image series; Tub, RFP-α-tubulin; Dyn, GFP$_2$-Dyn1). Elapsed time in seconds is given. Bar, 3 μm in overview and 1 μm in series. See also Supplemental Video material. (E) Examples of dynein rearrangement during MT motility. Before MT motion GFP$_2$-Dyn1 localizes to the plus-ends of short MTs. The dynein signal distributes along the length of the MT the moment when the polymer starts moving (arrows in E1) and returns to the plus-end when motility stops. Occasionally, dynein moves from one MT end to the other (arrow in E2). MT motility is often accompanied with the appearance of a stationary dynein signal (arrow in E3), suggesting that MTs slide over cortically anchored dynein. Tub, RFP-α-tubulin; Dyn, GFP$_2$-Dyn1. Elapsed time in seconds is given. Bars, 1 μm. Also see Supplemental Video material for Figure 6E1 and E3.

Dynein Is Required for Polarization of the Microtubule Array in Budding Cells

The described results suggested that MT translocation is based on dynein and that this motility participates in MT polarization. To gain further support for this notion, we next tested whether dynein is required for the rapid polarization of the MT array. We shifted the Peb1-YFP–expressing control strain FB2Peb1Y and the dynein mutant strain FB1Dyn2^{ts}_P1Y (Table 1) to 31–32°C for ~1 h, treated them with the solvent dimethyl sulfoxide (DMSO) or with benomyl, and monitored the polarization of the MT cytoskeleton after washout of the reagents (Figure 8A). Consistent with the previously described recovery experiments, control cells reestablished a polarized MT array within 4 min after removal of the drug (Figure 8A, black bars). In contrast, dynein mutants were already impaired in MT polarization and were almost unable to recover polarity of the MT array after benomyl treatment (Figure 8A, gray bars). We next asked whether inactivation of dynein affects the polarity of already established MT arrays. Quantitative analysis of Peb1-RFP

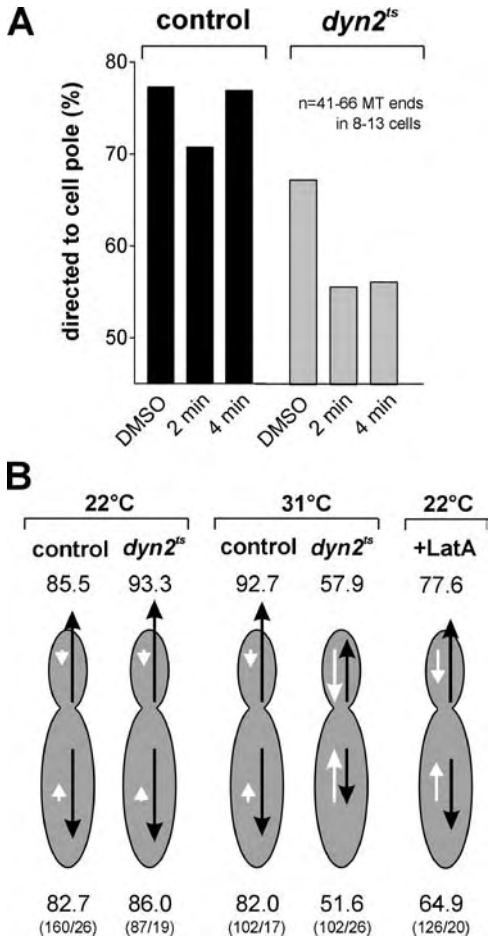

Figure 8. Role of dynein in microtubule polarization. (A) In benomyl recovery experiments at 31–32°C, cells of strain FB2Peb1Y (control) repolarized their MT array, with almost 80% of all MT plus-ends reaching to the distal pole of the mother cell (control). In contrast, dynein mutants (strain FB1Dyn2^{ts}_P1Y) were not able to repolarize their MT array after disruption of the MTs and washout of benomyl. Note that DMSO alone already slightly affects MT polarization. (B) Control cells (strain FB2Peb1R_GT) show normal MT polarization at both 22°C and after ~1 h in 31°C. In contrast, dynein mutants (FB1Dyn2^{ts}_P1R_GT) lose MT polarization after growth at restrictive temperature. A significant loss of MT polarization was also induced by disruption of F-actin with 20 μM LatA. Note that this correlates with the reduction of MT motility in LatA-treated control cells (see Figure 6B). Percentage of MT plus-ends growing to the cell poles is given above and below and is also indicated by size of black arrows; number of measurements/cell is given in parentheses.

motility in control cells (FB2Peb1R_GT) and dynein mutants (FB1Dyn2^{ts}_P1R_GT) revealed no difference at permissive temperature (Figure 8B, 22°C; number of signals/cell number is given in parentheses). After 70–90 min at restrictive temperature, MT arrays in control cells were still polarized (31°C, control). In contrast, MT polarity was almost lost in dynein mutants (Figure 8B, 31°C, dyn2ts). These results added further support to the notion that dynein activity is essential to maintain a polarized MT array in budding cells, and this could be a consequence of reduced MT motility. To get further support for this idea, we disrupted the F-actin, a treatment that was shown to reduce MT motility (Figure 7B). After treatment with latrunculin A for 1 h at 22°C, MT polarization was significantly affected, which was most obvious in mother cells (Figure 8B, compare 64.9% polarized in mother cell in +LatA to 82.7% polarized in mother cells of control at 22°C). Together, these data are most consistent with a role of dynein-dependent MT motility in polarization of the MT array.

DISCUSSION

Microtubules Are Nucleated by Cytoplasmic γ-Tubulin–containing Nucleation Sites

In unbudded cells of *U. maydis*, numerous cytoplasmic MTOCs form an antipolar MT array (Straube *et al.*, 2003). On bud formation, the tubulin cytoskeleton is thought to polarize due to the activity of MTOCs in the neck region that send MTs out into the mother and the daughter cells (Steinberg *et al.*, 2001; Straube *et al.*, 2003). Here, we show that these polar MTOCs consist of numerous smaller γ-tubulin–containing sites that show directional motility within the cell. It was previously reported that ~85% of all MT plus-ends, labeled with an EB1-homologue, grow toward the distal cell pole, whereas ~15% of the MTs had an opposite orientation (Straube *et al.*, 2003). A more detailed analysis revealed that the polarity of the array is based on the long MTs that are bound to the neck, whereas the free and motile MTs have a random orientation (Figure 1D), suggesting that these MTs are not yet focused at the neck region. In *U. maydis*, MTs rapidly move through the cytoplasm (Steinberg *et al.*, 2001; this study), and most of them were associated with γ-tubulin-GFP dots, suggesting that nucleation sites and associated MTs are transported. This idea is supported by the benomyl recovery experiments, in which the nucleation sites lost their polar localization and were randomly distributed within the cytoplasm, where they most likely nucleate the reappearing MTs. Moreover, both polar localization of the MTOCs and polarity of the array are rapidly restored. Thus, bipolar cytoplasmic nucleation sites organize the MT array not only in unbudded cells (Straube *et al.*, 2003) but also during budding, where the MTOCs are concentrated in the neck region (Figure 9). Cytoplasmic nucleation has also been described for animal systems (Yvon and Wadsworth, 1997; Vorobjev *et al.*, 1997), and we therefore consider it likely that this mechanism of MT organization might be more common than anticipated.

Transport of Microtubules in U. maydis *Depends on Dynein*

In *U. maydis*, MTs undergo bending and rapid directed motility (Steinberg *et al.*, 2001). Motility of free MTs could result from elongation at one end, while the other end is shrinking at similar rates, a mechanism known as treadmilling (Margolis and Wilson, 1981; Rodionov and Borisy, 1997a). Most interestingly, this mechanism has the potential to organize MT arrays in a polar manner (Maly and Borisy, 2002) and might therefore participate in MT organization in *U. maydis*. However, MT motility happens at average rates of 30–42 μm/min (Steinberg *et al.*, 2001), which is in the range of motor activity but much faster than the observed MT elongation rate of ~10 μm/min (Steinberg *et al.*, 2001; Adamikova *et al.*, 2004). Moreover, our speckle analysis strongly argues against MT treadmilling but supports the notion that assembled MTs are transported by molecular motors. MT motility has been described in animal systems (Seitz-Tutter *et al.*, 1988; Tanaka and Kirschner, 1991; Keating *et al.*, 1997; Dent *et al.*, 1999; Yu *et al.*, 2001) and in the ameba *Dictyostelium discoideum* (Koonce *et al.*, 1999; Brito *et al.*, 2005), but it is not known for other fungi. According to

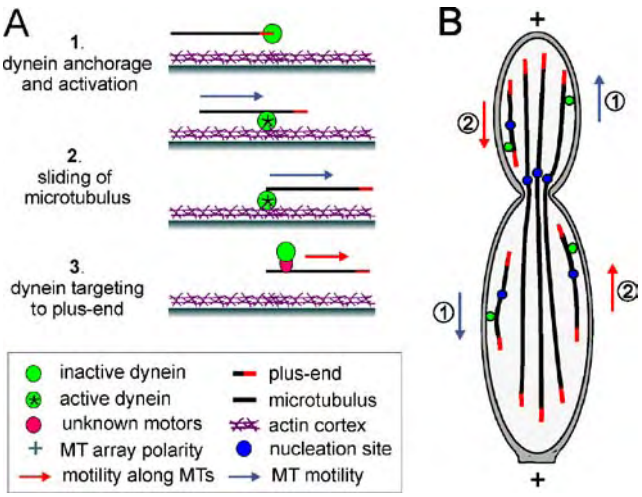

Figure 9. Model of the mechanism of dynein-dependent in MT polarization in *U. maydis*. (A) Mechanism of cortical MT sliding. Dynein localizes to MT plus-ends. Before MT motility it is anchored to the cell cortex and becomes activated (1). Due to the stable interaction of the motor with the cell cortex, the MT itself slides along the cortex (2). Subsequently, unknown plus-motors take dynein back to the MT plus-end (3). Note that F-actin independent MT motility mechanisms exist. (B) Model of the role of dynein in MT polarization in *U. maydis*. MTs are mainly nucleated by numerous cytoplasmic nucleation sites at the neck region and extend their plus-ends toward both cell poles. Dynein at the cell cortex transports assembled MTs and associated γ-tubulin–containing nucleation sites toward the neck region (1), where they are held in place by an unknown mechanism. In addition, dynein pulls on MTs toward the cell poles, so that they are straightened in the cell. This activity occasionally overcomes the anchorage of MTs at the neck and drags MTs and nucleation sites out of the neck and toward the poles (2). For the sake of simplicity, dynein at MT plus-ends is not depicted.

the "sliding filament model," cytoplasmic dynein in the axon is anchored at the cortex and pushes MTs with their plus-end leading toward the synapsis (Ahmad *et al*., 1998; Hasaka *et al*., 2004; He *et al*., 2005), thereby orienting MTs within the axon (Baas and Buster, 2004). A similar situation might exist in *U. maydis*. In vivo observation of MT plus-ends, labeled with an EB1-homologue, indicated that most motility is driven by a minus-motor. Indeed, MT motility was almost abolished in dynein mutants, suggesting that this minus-motor is responsible for MT motility in the fungus *U. maydis*. In neurons, it is thought that dynein-based MT motility requires the anchorage of the motor to the cell cortex, which is most likely mediated by cortical F-actin (Hasaka *et al*., 2004). Interestingly, treatment with the anti-actin reagent latrunculin A inhibited only ~50% of the dynein-driven MT transport in *U. maydis*, suggesting that a significant portion of the observed motility occurs independently of cortical F-actin. Latrunculin-insensitive motility of individual MTs was also reported in *D. discoideum* (Brito *et al*., 2005), which argues that cortex-independent motility of assembled tubulin is a general phenomenon.

Dynein Translocates along the Moving Microtubule

In fungi, it was shown that dynein localizes to the plus-ends of MTs (Sheeman *et al*., 2003; Zhang *et al*., 2003), where it is thought to be stored in an inactive form until it becomes activated for minus-end–directed motility. The best-known example for this is spindle motility in *Saccharomyces cerevisiae*. Here, growing MTs take dynein to the cell cortex, where it becomes "off loaded" and activated, which results in sliding of the astral MT along the stationary dynein (Heil-Chapdelaine *et al*., 2000; Lee *et al*., 2003, 2005; Sheeman *et al*., 2003). Our results on dynein localization in *U. maydis* argue for a similar mechanism in motility of interphase MTs. In this model, inactive dynein is stored at MT plus-ends. On activation, it is anchored to a cellular matrix, such as the cortical actin and moves to the minus-end of the free MT, which results in sliding of the filament along the stationary motor (Figure 9A). The inhibition of MT motility by LatA adds support to such a model. Motility is followed by plus-end targeting of dynein, which delivers the minus-motor back to the MT tip for another round of motility.

A Model of Dynein Function in Organizing the MT Array in U. maydis

The results summarized here demonstrate that MT organization in *U. maydis* is a complex process that involves cytoplasmic nucleation sites, MTs, and dynein. MTs and associated γ-tubulin–containing nucleation sites move throughout the cytoplasm by the activity of dynein, which is required to maintain the MT array polarized. Thus, it is most likely that dynein activity takes nucleation sites toward the neck, thereby arranging the MT cytoskeleton (Figure 9B). However, motility of MTs and nucleation sites was also directed toward the cell poles (Figures 4A and 9B, 2), suggesting that dynein also exerts outward forces on the MT array. In *U. maydis*, MTs are often bundled and extend straight from the neck to the cell poles (Steinberg *et al*., 2001). Plus- and minus-motors exert forces on these MTs (Straube *et al*., 2006; this study), indicating that the regular organization of the array is a consequence of counteracting motor activity. Thus, poleward dynein activity might primarily stretch MTs into the cell body (Figure 9B, 1), while counteracting MT-based forces focus bipolar nucleation sites at the neck region, where MT bundling forces stabilize them. This idea is supported by the observation that polar accumulation of nucleation sites is abolished in the absence of MTs, suggesting that interaction between MTs is required for keeping the MTOCs at the neck.

In conclusion, our work further supports a concept in which motor proteins organize the MT array, and this process is conserved from neurons (Sharp *et al*., 1997b; Ahmad *et al*., 1998; Yu *et al*., 2000) to fungi (Carazo-Salas *et al*., 2005; Straube *et al*., 2006; this study). Our data show that MT organization in *U. maydis* is based on a complex interplay of MT nucleation at cytoplasmic sites and molecular motors. It is presently unknown whether dynein directly transports nucleation sites or supports their assembly. However, our results make it likely that MT motility participates in polarizing of the MT array. Although further studies are needed to elucidate the mechanistic details, our data indicate that the capacity of motor-based self-organization of MTs is conserved from animals to fungi.

ACKNOWLEDGMENTS

We thank Daniela Aßmann for technical help and Anne Straube and Ulrike Theisen for improving the manuscript. We also thank the anonymous referees for constructive criticism that greatly helped improve the article. This work was supported by Deutsche Forschungsgemeinschaft STE 799/4-2 and the Max Planck Gesellschaft.

REFERENCES

Adamikova, L., Straube, A., Schulz, I., and Steinberg, G. (2004). Calcium signaling is involved in dynein-dependent microtubule organization. Mol. Biol. Cell *15*, 1969–1980.

Ahmad, F. J., Echeverri, C. J., Vallee, R. B., and Baas, P. W. (1998). Cytoplasmic dynein and dynactin are required for the transport of microtubules into the axon. J. Cell Biol. *140*, 391–401.

Baas, P. W., and Ahmad, F. J. (1993). The transport properties of axonal microtubules establish their polarity orientation. J. Cell Biol. *120*, 1427–1437.

Baas, P. W., and Buster, D. W. (2004). Slow axonal transport and the genesis of neuronal morphology. J. Neurobiol. *58*, 3–17.

Banuett, F., and Herskowitz, I. (1989). Different *a* alleles of *Ustilago maydis* are necessary for maintenance of filamentous growth but not for meiosis. Proc. Natl. Acad. Sci. USA *86*, 5878–5882.

Barral, D. C., and Seabra, M. C. (2004). The melanosome as a model to study organelle motility in mammals. Pigment Cell Res. *17*, 111–118.

Bottin, A., Kamper, J., and Kahmann, R. (1996). Isolation of a carbon source-regulated gene from *Ustilago maydis*. Mol. Gen. Genet. *253*, 342–352.

Brito, D. A., Strauss, J., Magidson, V., Tikhonenko, I., Khodjakov, A., and Koonce, M. P. (2005). Pushing forces drive the comet-like motility of microtubule arrays in *Dictyostelium*. Mol. Biol. Cell *16*, 3334–3340.

Burkhardt, J. K. (1998). The role of microtubule-based motor proteins in maintaining the structure and function of the Golgi complex. Biochim. Biophys. Acta *1404*, 113–126.

Campbell, R. E., Tour, O., Palmer, A. E., Steinbach, P. A., Baird, G. S., Zacharias, D. A., and Tsien, R. Y. (2002). A monomeric red fluorescent protein. Proc. Natl. Acad. Sci. USA *99*, 7877–7882.

Carazo-Salas, R. E., Antony, C., and Nurse, P. (2005). The kinesin Klp2 mediates polarization of interphase microtubules in fission yeast. Science *309*, 297–300.

Dent, E. W., Callaway, J. L., Szebenyi, G., Baas, P. W., and Kalil, K. (1999). Reorganization and movement of microtubules in axonal growth cones and developing interstitial branches. J. Neurosci. *19*, 8894–8908.

Desai, A., and Mitchison, T. J. (1997). Microtubule polymerization dynamics. Annu. Rev. Cell Dev. Biol. *13*, 83–117.

Fuchs, U., Manns, I., and Steinberg, G. (2005). Microtubules are dispensable for the initial pathogenic development but required for long-distance hyphal growth in the corn smut fungus *Ustilago maydis*. Mol. Biol. Cell *16*, 2746–2758.

Gadde, S., and Heald, R. (2004). Mechanisms and molecules of the mitotic spindle. Curr. Biol. *14*, R797–R805.

Garces, J. A., Clark, I. B., Meyer, D. I., and Vallee, R. B. (1999). Interaction of the p62 subunit of dynactin with Arp1 and the cortical actin cytoskeleton. Curr. Biol. *9*, 1497–1500.

Gross, S. P., Tuma, M. C., Deacon, S. W., Serpinskaya, A. S., Reilein, A. R., and Gelfand, V. I. (2002). Interactions and regulation of molecular motors in *Xenopus* melanophores. J. Cell Biol. *156*, 855–865.

Hasaka, T. P., Myers, K. A., and Baas, P. W. (2004). Role of actin filaments in the axonal transport of microtubules. J. Neurosci. *24*, 11291–11301.

Heil-Chapdelaine, R. A., Oberle, J. R., and Cooper, J. A. (2000). The cortical protein Num1p is essential for dynein-dependent interactions of microtubules with the cortex. J. Cell Biol. *151*, 1337–1344.

He, Y., Francis, F., Myers, K. A., Yu, W., Black, M. M., and Baas, P. W. (2005). Role of cytoplasmic dynein in the axonal transport of microtubules and neurofilaments. J. Cell Biol. *168*, 697–703.

Hirokawa, N. (1998). Kinesin and dynein superfamily proteins and the mechanism of organelle transport. Science *279*, 519–526.

Holliday, R. (1974). *Ustilago maydis*. In: Handbook of Genetics, ed. R. C. King, New York: Plenum Press.

Karki, S., and Holzbaur, E. L. (1999). Cytoplasmic dynein and dynactin in cell division and intracellular transport. Curr. Opin. Cell Biol. *11*, 45–53.

Karsenti, E., and Vernos, I. (2001). The mitotic spindle: a self-made machine. Science *294*, 543–547.

Keating, T. J., Peloquin, J. G., Rodionov, V. I., Momcilovic, D., and Borisy, G. G. (1997). Microtubule release from the centrosome. Proc. Natl. Acad. Sci. USA *94*, 5078–5083.

Koonce, M. P., Kohler, J., Neujahr, R., Schwartz, J. M., Tikhonenko, I., and Gerisch, G. (1999). Dynein motor regulation stabilizes interphase microtubule arrays and determines centrosome position. EMBO J. *18*, 6786–6792.

Lane, J., and Allan, V. (1998). Microtubule-based membrane movement. Biochim. Biophys. Acta *1376*, 27–55.

Lane, J. D., and Allan, V. J. (1999). Microtubule-based endoplasmic reticulum motility in *Xenopus laevis*: activation of membrane-associated kinesin during development. Mol. Biol. Cell *10*, 1909–1922.

Lee, W. L., Kaiser, M. A., and Cooper, J. A. (2005). The offloading model for dynein function: differential function of motor subunits. J. Cell Biol. *168*, 201–207.

Lee, W. L., Oberle, J. R., and Cooper, J. A. (2003). The role of the lissencephaly protein Pac1 during nuclear migration in budding yeast. J. Cell Biol. *160*, 355–364.

Lippincott-Schwartz, J. (1998). Cytoskeletal proteins and Golgi dynamics. Curr. Opin. Cell Biol. *10*, 52–59.

Lippincott-Schwartz, J., Cole, N. B., Marotta, A., Conrad, P. A., and Bloom, G. S. (1995). Kinesin is the motor for microtubule-mediated Golgi-to-ER membrane traffic. J. Cell Biol. *128*, 293–306.

Maly, I. V., and Borisy, G. G. (2002). Self-organization of treadmilling microtubules into a polar array. Trends Cell Biol. *12*, 462–465.

Mandelkow, E., and Mandelkow, E. M. (1995). Microtubules and microtubule-associated proteins. Curr. Opin. Cell Biol. *7*, 72–81.

Margolis, R. L., and Wilson, L. (1981). Microtubule treadmills–possible molecular machinery. Nature *293*, 705–711.

Mogensen, M. M. (1999). Microtubule release and capture in epithelial cells. Biol. Cell *91*, 331–341.

Rodionov, V. I., and Borisy, G. G. (1997a). Microtubule treadmilling in vivo. Science *275*, 215–218.

Rodionov, V. I., and Borisy, G. G. (1997b). Self-centering activity of cytoplasm. Nature *386*, 170–173.

Schulz, B., Banuett, F., Dahl, M., Schlesinger, R., Schafer, W., Martin, T., Herskowitz, I., and Kahmann, R. (1990). The *b* alleles of *U. maydis*, whose combinations program pathogenic development, code for polypeptides containing a homeodomain-related motif. Cell *60*, 295–306.

Seitz-Tutter, D., Langford, G. M., and Weiss, D. G. (1988). Dynamic instability of native microtubules from squid axons is rare and independent of gliding and vesicle transport. Exp. Cell Res. *178*, 504–512.

Sharp, D. J., Kuriyama, R., Essner, R., and Baas, P. W. (1997a). Expression of a minus-end-directed motor protein induces Sf9 cells to form axon-like processes with uniform microtubule polarity orientation. J. Cell Sci. *110*, 2373–2380.

Sharp, D. J., Rogers, G. C., and Scholey, J. M. (2000). Roles of motor proteins in building microtubule-based structures: a basic principle of cellular design. Biochim. Biophys. Acta *1496*, 128–141.

Sharp, D. J., Yu, W., Ferhat, L., Kuriyama, R., Rueger, D. C., and Baas, P. W. (1997b). Identification of a microtubule-associated motor protein essential for dendritic differentiation. J. Cell Biol. *138*, 833–843.

Sheeman, B., Carvalho, P., Sagot, I., Geiser, J., Kho, D., Hoyt, M. A., and Pellman, D. (2003). Determinants of *S. cerevisiae* dynein localization and activation: implications for the mechanism of spindle positioning. Curr. Biol. *13*, 364–372.

Steinberg, G., Wedlich-Soldner, R., Brill, M., and Schulz, I. (2001). Microtubules in the fungal pathogen *Ustilago maydis* are highly dynamic and determine cell polarity. J. Cell Sci. *114*, 609–622.

Straube, A., Brill, M., Oakley, B. R., Horio, T., and Steinberg, G. (2003). Microtubule organization requires cell cycle-dependent nucleation at dispersed cytoplasmic sites: polar and perinuclear microtubule organizing centers in the plant pathogen *Ustilago maydis*. Mol. Biol. Cell *14*, 642–657.

Straube, A., Enard, W., Berner, A., Wedlich-Soldner, R., Kahmann, R., and Steinberg, G. (2001). A split motor domain in a cytoplasmic dynein. EMBO J. *20*, 5091–5100.

Straube, A., Hause, G., Fink, G., and Steinberg, G. (2006). Conventional kinesin mediates microtubule-microtubule interactions *in vivo*. Mol. Biol. Cell *17*, 907–916.

Tanaka, E. M., and Kirschner, M. W. (1991). Microtubule behavior in the growth cones of living neurons during axon elongation. J. Cell Biol. *115*, 345–363.

Vale, R. D. (2003). The molecular motor toolbox for intracellular transport. Cell *112*, 467–480.

Vorobjev, I. A., Svitkina, T. M., and Borisy, G. G. (1997). Cytoplasmic assembly of microtubules in cultured cells. J. Cell Sci. *110*, 2635–2645.

Wedlich-Soldner, R., Schulz, I., Straube, A., and Steinberg, G. (2002a). Dynein supports motility of endoplasmic reticulum in the fungus *Ustilago maydis*. Mol. Biol. Cell *13*, 965–977.

Wedlich-Soldner, R., Straube, A., Friedrich, M. W., and Steinberg, G. (2002b). A balance of KIF1A-like kinesin and dynein organizes early endosomes in the fungus *Ustilago maydis*. EMBO J. *21*, 2946–2957.

Yu, W., Centonze, V. E., Ahmad, F. J., and Baas, P. W. (1993). Microtubule nucleation and release from the neuronal centrosome. J. Cell Biol. *122*, 349–359.

Yu, W., Cook, C., Sauter, C., Kuriyama, R., Kaplan, P. L., and Baas, P. W. (2000). Depletion of a microtubule-associated motor protein induces the loss of dendritic identity. J. Neurosci. *20*, 5782–5791.

Yu, W., Ling, C., and Baas, P. W. (2001). Microtubule reconfiguration during axogenesis. J. Neurocytol. *30*, 861–875.

Yu, W., Sharp, D. J., Kuriyama, R., Mallik, P., and Baas, P. W. (1997). Inhibition of a mitotic motor compromises the formation of dendrite-like processes from neuroblastoma cells. J. Cell Biol. *136*, 659–668.

Yvon, A. M., and Wadsworth, P. (1997). Non-centrosomal microtubule formation and measurement of minus end microtubule dynamics in A498 cells. J. Cell Sci. *110*, 2391–2401.

Zhang, J., Li, S., Fischer, R., and Xiang, X. (2003). Accumulation of cytoplasmic dynein and dynactin at microtubule plus ends in *Aspergillus nidulans* is kinesin dependent. Mol. Biol. Cell *14*, 1479–1488.